CHEMISTRY OF MATERIALS
Article

Chem. Mater. **2009,** *21,* 4859–4867 4859
DOI:10.1021/cm901463u

Organic−Organic Heteroepitaxy of Semiconductor Crystals: α-Quaterthiophene on Rubrene

Marcello Campione,* Luisa Raimondo, Massimo Moret, Paolo Campiglio, Enrico Fumagalli, and Adele Sassella

Department of Materials Science & CNISM, University of Milano Bicocca, Via Cozzi 53, I-20125 Milan, Italy

Received May 28, 2009. Revised Manuscript Received August 25, 2009

Organic−organic epitaxy is a successful strategy for growing highly oriented and crystalline heterojunctions of organic semiconductors. Within this class of materials, crystalline rubrene is especially promising because of its outstanding hole mobility. Here, the (200) surface of rubrene single crystals was used as substrate for growing thin films of another organic semiconductor: α-quaterthiophene. The film growth proceeds via a 3D mechanism, with the formation of a few-monolayer-thick crystalline islands oriented along two main directions, as deduced by the optical reflection of the α-quaterthiophene/rubrene heterostructure measured over macroscopic regions. An atomic-scale analysis of the film surface performed with scanning force microscopy revealed a complete textural order achieved through a line-on-line epitaxial relation. With the help of empirical force-field calculations of the heteroepitaxial interface, this orienting propensity is demonstrated to be strictly related to the peculiar corrugation of the rubrene crystal surface, showing marked furrows along two orthogonal crystallographic directions.

1. Introduction

A large variety of organic molecules bearing a π-conjugated system have been demonstrated to form crystalline phases with a semiconducting behavior.[1] The ability to transport charges originates from the $\pi-\pi$ interactions established in the solid, giving rise to an electronic structure typical of semiconductors. On the other hand, these interactions are the major driving force for the assembly of the crystalline molecular solid, especially in the case of organic semiconductors containing only C- and H-atoms. Rubrene (RUB, $C_{42}H_{28}$, 5,6,11,12-tetraphenyltetracene) and pentacene are the most studied and promising materials falling in this category. Both of them bear a rigid π-conjugated system constituted by an oligocene core; however, RUB is not a simple rodlike molecule, because it possesses also four lateral phenyl substituents. The interactions among the conjugate cores give rise to crystalline phases with layered herringbone structures for most rodlike molecules, with the herringbone plane almost perpendicular to the main molecular axes.[2] For RUB, in its orthorhombic phase the herringbone motif is retained, but the herringbone plane is parallel to the main molecular axis.[3] This structure confers a particularly favorable overlap of π-orbitals along the [020] crystallographic direction, determining, along that direction, a relatively high charge mobility.[4]

Besides the interest to study the intrinsic properties of organic semiconductors, recent results demonstrated the advantages from an applicative standpoint reachable through the combination of different materials in multilayer heterojunctions.[5,6] Organic molecular beam epitaxy (OMBE) is particularly amenable to the problem of growing heterostructures with controlled morphology and structure. This technique requires the selection of a crystalline substrate that templates the growth of the first organic overlayer; the way the substrate drives the assembly of deposited molecules is generally expressed by the term epitaxy. Although in inorganic semiconductors epitaxy is substantially determined by the geometric match between substrate and overlayer lattice points favoring the formation of strong atomic bonds, in organic semiconductors, other subtle mechanisms may be active. In particular, it was observed that even when lattice match is completely absent, i.e., the matrix transforming the substrate lattice vectors into those of the overlayer has noninteger and/or irrational elements, the growth of an overlayer with preferential orientations may occur.

*Corresponding author. Address: Department of Geological Sciences and Geotechnologies and CNISM, University of Milano Bicocca, Piazza della Scienza 4, I-20126 Milan, Italy. E-mail: marcello.campione@unimib.it. Tel: +39 02 64482089. Fax: +39 02 64482073.

(1) Brütting, W. *Physics of Organic Semiconductors*; Wiley-VCH: Weinheim, Germany, 2005.
(2) Fichou, D. *J. Mater. Chem.* **2000**, *10*, 571.
(3) Jurchescu, O. D.; Meetsma, A.; Palstra, T. T. M. *Acta Crystallogr., Sect. B* **2006**, *B62*, 330.
(4) Podzorov, V.; Menard, E.; Borissov, A.; Kiryukhin, V.; Rogers, J. A; M. Gershenson, E. *Phys. Rev. Lett.* **2004**, *93*, 086602.
(5) Chu, C .-W.; Shao, Y.; Shrotriya, V.; Yang, Y. *Appl. Phys. Lett.* **2005**, *86*, 243506.
(6) Pandey, A. K.; Nunzi, J.;-M. *Adv. Mater.* **2007**, *19*, 3613.
(7) Campione, M.; Sassella, A.; Moret, M.; Papagni, A.; Trabattoni, S.; Resel, R.; Lengyel, O.; Marcon, V.; Raos, G. *J. Am. Chem. Soc.* **2006**, *128*, 13378.

Published on Web 09/30/2009

This situation is encountered mostly in organic−organic interfaces.[7−12] The investigation of the mechanisms responsible for the orientation effect of an organic substrate to an organic overlayer is foundational for the development of a technology exploiting multilayer heterojunctions.

Here, we report a paradigmatic example of epitaxy of organic semiconductors represented by the heterojunction formed by depositing α-quaterthiophene (α-4T) on the surface of a single crystal of RUB. Orthorhombic RUB single crystals (a = 26.86 Å b = 7.19 Å, and c = 14.43 Å)[3] can be easily grown as thin slabs exposing a large, atomically flat (200) surface that is used as substrate for depositing α-4T by OMBE; α-4T crystallizes in (002)-oriented monoclinic domains with the structure of one of the known polymorphs (a = 6.09 Å b = 7.86 Å, and c = 30.48 Å, β = 91.8 Å).[13] Despite the apparent geometrical incommensurism between the surface lattices of the two materials, the macroscopic analysis of the optical properties of the α-4T/RUB heterostructures reveals a clear preferential orientation of the α-4T film with respect to the RUB substrate, indicating heteroepitaxial growth. Atomic-scale imaging performed with atomic force microscopy (AFM) reveals the presence of four rotationally equivalent domains with the same line-on-line epitaxial relation with the substrate; this relation is then rationalized in terms of interface symmetry and adhesive interactions arising from the peculiar corrugation of the RUB(200) and α-4T(002) surfaces. In addition, validation of these results is obtained from empirical force field calculations performed starting from the bulk, nonreconstructed, surface structure of the two materials. The critical comparison of all the different experimental results provides a complete picture of these paradigmatic heterostructures, which are demonstrated to be grown epitaxially, with a nonequivalent population of the observed four orientations of the crystalline domains.

2. Experimental Procedures and Methods

RUB single crystals were grown by physical vapor transport.[14] Lath-shaped single crystals[15] were selected for the deposition experiments since they exhibit atomically flat singular (200) surfaces, with single terraces extending over distances as large as 50 μm. Because of their low thickness, single crystals adhere spontaneously on polished glass plates, which were used as mechanical supports. The deposition of α-4T was carried out by OMBE working under an ultrahigh vacuum with a Knudsen-type effusion cell and the film thickness was monitored with a quartz crystal microbalance.

Polarized optical reflection measurements were carried out in the spectral range from 2 to 6 eV using a Perkin-Elmer Lambda900 spectrometer with a depolarizer and Glan-Taylor polarizers, equipped with a near normal incidence reflection accessory: all the spectra have been corrected for the instrumental response. The axis directions of RUB single crystals used as substrates have been located with an uncertainty of ±1°. The light spot size used during the experiments (a few square millimeters) allowed significant statistical analysis over a macroscopic sample area.

AFM measurements were performed with a Nanoscope IIIa MultiMode (Digital Instruments) under a dry nitrogen atmosphere, using silicon nitride tips (Veeco ORC8, force constant 0.05 N/m) for transverse shear microscopy (TSM)[16] measurements and atomic-scale imaging, and using silicon tips (Veeco RTESP, force constant 40 N/m, resonance frequency 250 kHz) for intermittent-contact mode imaging.

Computer simulations of possible epitaxial relationships between an α-4T(002) overlayer and a RUB(200) substrate were based on atom−atom empirical potentials[17] fed to a locally modified version of the AutoDock3 molecular docking package.[18] The azimuthal dependence of the system potential energy of an α-4T(002) slab sitting on a bulk terminated RUB(200) surface was studied. The simulation box comprised 351^3 grid points (corresponding to a sampling grid of 0.217 Å) and mapped the interaction potential between substrate and epitaxial crystallites. The RUB(200) substrate was modeled as a slab of 1 × 18 × 9 unit cells along the a, b, and c axes, respectively, giving rise to a total of 629 molecules. The α-4T(002) monolayer crystallite was modeled as 39 herringbone packed molecules, with a total of 3446 docking runs, giving a satisfactory sampling statistics of the in-plane orientations of the overlayer crystallites. Approximate energy minima values found with AutoDock3 were improved by minimization with program Orient 4.6.11 using the same interaction potentials.[19]

3. Results and Discussion

Our experimental approach is based on the exploitation of the complementary features of optical spectroscopy and scanning probe techniques. Indeed, the optical analysis, besides giving information on the intrinsic optical properties of the organic heterostructures,[12,20] allows one to achieve statistical consistency of the measured sample response but with some limitations on the possibility to define accurately and univocally epitaxial relations. This gap is filled by scanning probe analysis performed at the atomic-scale, which suffers some inadequacy at collecting data with sufficient statistical relevancy.

(8) Marcon, V.; Raos, G.; Campione, M.; Sassella, A. *Cryst. Growth Des.* **2006**, *6*, 1826.
(9) Sassella, A.; Campione, M.; Borghesi, A. *Riv. Nuovo Cimento* **2008**, *81*, 257.
(10) Mannsfeld, S. C. B.; Leo, K.; Fritz, T. *Phys. Rev. Lett.* **2005**, *94*, 056104.
(11) Mannsfeld, S. C. B.; Leo, K.; Fritz, T. *Mod. Phys. Lett. B* **2006**, *20*, 585.
(12) Forker, R.; Kasemann, D.; Dienel, T.; Wagner, C.; Franke, R.; Müllen, K.; Fritz, T. *Adv. Mater.* **2008**, *20*, 4450.
(13) Siegrist, T.; Kloc, Ch.; Laudise, R. A.; Katz, H. E.; Haddon, R. C. *Adv. Mater.* **1998**, *10*, 379.
(14) Laudise, R. A.; Kloc, Ch.; Simpkins, P. G.; Siegrist, T. *J. Cryst. Growth* **1998**, *187*, 449.
(15) Zeng, X.; Zhang, D.; Duan, L.; Wang, L.; Dong, G.; Qiu, Y. *Appl. Surf. Sci.* **2007**, *253*, 6047.
(16) Puntambekar, K.; Dong, J.; Haugstad, G.; Frisbie, C. D. *Adv. Funct. Mater.* **2006**, *16*, 879.
(17) Gavezzotti, A. *Molecular Aggregation: Structure Analysis and Molecular Simulation of Crystals and Liquids*; Oxford University Press: New York, 2007; p 215.
(18) Morris, G. M.; Goodsell, D. S.; Halliday, R. S.; Huey, R.; Hart, W. E.; Belew, R. K.; Olson, A. J. *J. Comput. Chem.* **1998**, *19*, 1639.
(19) Stone, A. J.; Dullweber, A.; Engkvist, O.; Fraschini, E.; Hodges, M. P.; Meredith, A. W.; Nutt, D. R.; Popelier, P. L. A.; Wales, D. J. *Orient: A Program for Studying Interactions between Molecules*, version 4.6; University of Cambridge: Cambridge, U.K., 2002. Enquiries to A. J. Stone, ajs1@cam.ac.uk.
(20) Sassella, A.; Campione, M.; Raimondo, L.; Borghesi, A.; Bussetti, G.; Cirilli, S.; Violante, A.; Goletti, C.; Chiaradia, P. *Appl. Phys. Lett.* **2009**, *94*, 073307.

In the following, a brief description of the heterostructure morphology over micrometric-scales is provided at first. A complete picture of the macroscopic optical response of the heterostructure under polarized light is then presented, deducing fundamental structural characteristics of the sample. Finally, the results of the microscopic analysis performed with AFM and empirical force field calculations are presented, showing the consistency with optical results and providing the necessary accuracy for identifying the epitaxial relations and the orientation mechanism of the overlayer.

3.1. Morphology and Macroscopic Properties. For studying the film morphology and its evolution with coverage over regions of the sample surface of the order of 1×10^2 to 1×10^3 μm^2, we have monitored ex-situ with AFM the same area of a sample after sequentially depositing on it 1, 5, and 10 nm of α-4T. One-nanometer-thick samples (Figure 1a, d, and g, and Figure 2a) show the presence of elongated islands with uniform height, distributed within the range 4.6 ± 1.2 nm. Each island appears with a fringed edge developing along the crystallographic directions RUB[021] or RUB[02$\bar{1}$] (therefore forming an angle of 89.80° with one another), which are also the directions of elongation of the islands. The flat top of the islands gives an indication of their crystallinity, while their height, as measured in 1 nm thick samples, suggests that they are (002)-oriented domains of the low-temperature polymorph of α-4T (on average 3 monomolecular layer thick, with $d_{002} = 1.53$ nm).[13] By incrementing the film thickness up to 5 nm (Figure 1b, e, and h, and Figure 2b), the islands are observed to increase only in their lateral size, while displaying a more compact shape, then giving rise to a quite uniform layer. In 10 nm thick films (Figure 1c, f, and i, and Figure 2c), the island height is observed to increase to reach approximately the nominal film thickness, whereas the substrate coverage remains unvaried. This anisotropy of the growth rates reflects the anisotropy of molecular interactions: the edges of already-formed α-4T crystal domains appear to be preferential sites for the adsorption of diffusing molecules, whereas the aggregation of incoming molecules on the molecularly flat top surface of islands starts only when an almost complete coverage is reached. On the basis of these observations, the growth mode of α-4T on RUB deposited by OMBE is clearly Volmer−Weber.

The study of the optical properties of the α-4T/RUB heterostructure is addressed to relate the preferential growth directions of islands to its macroscopic behavior. Reflection spectroscopy under polarized light was performed rather than transmission because absorption of RUB single crystals at normal incidence on RUB(200) in the ultraviolet spectral range is particularly strong,[21] so that it prevents the full detection of the absorption features even for few hundreds nm thick single crystals.

The reflectance spectra collected in the energy range from 2.1 to 5.9 eV on the bare RUB single crystal used as substrate and on the complete heterostructure with 10 nm of α-4T are reported in Figure 3a−b for different light polarization, labeled by the angle δ between the direction of the electric field of the incident light and RUB[010]. This latter direction is a reference direction for the optical response of the RUB single crystal.[21] The sharp edge detected at about 2.2 eV identifies the absorption edge of RUB single crystal. Indeed, because of the finite thickness of the RUB single crystal and to its low absorption coefficient at energy lower than 3.4 eV, the incident light is reflected from the back-side of the sample after having crossed the whole crystal thickness. The same edge is detected in the spectra in Figure 3b since the α-4T absorption edge lies at higher energy (about 2.6 eV).[22,23] After the deposition of α-4T, a strong modification of the spectral line shape and intensity as well as of the optical anisotropy with respect to the bare RUB substrate is detected at energy higher than 3.5 eV, whereas at lower energy the spectral line shape and the related intensity is almost unchanged. In particular, after deposition the peaks at 4.0 and 4.3 eV in the $\delta = 0°$ spectra undergo an intensity decrease and a shift; those at about 3.7 and 4.1 eV in the $\delta = 90°$ spectra display some intensity decrease.

For a better visualization of the contribution of the α-4T overlayer, the difference spectra ΔR_{exp} between couples of reflectance spectra, collected in the same polarization configuration on the heterostructure and on the bare RUB substrate, are reported in Figure 4 for different δ values. The ΔR_{exp} spectra are reported in the energy range between 2.6 and 4.3 eV, where the α-4T single crystal response is known to display a strong optical anisotropy,[22,23] which can therefore be expected to be observed. Even though the difference between reflectance spectra can not give the actual optical response of the lone overlayer,[24] it gives nonetheless important information.

We observe that the ΔR_{exp} spectra evolve with the angle of polarization δ, thus evidencing an intrinsic anisotropy of the α-4T overlayer; the two extremes clearly coincide with $\delta = 0$ and 90°. For $\delta = 0°$ the spectrum ΔR_{exp} displays a maximum at about 3.6−3.7 eV, thus resembling the spectral line shape of α-4T[100] polarized reflectance collected on the α-4T(002) face of a bulk crystal;[23] on the contrary, for $\delta = 90°$ an almost flat spectral line shape characterizes the ΔR_{exp} spectrum in the same range, as indeed expected in the α-4T[100]-polarized optical response.[22] At higher energy, the contribution of the α-4T/RUB interface starts being detected and the interpretation of ΔR_{exp} becomes less straightforward (see the Supporting Information, Figure S1). From Figure 4 the following conclusions can be drawn.

(21) Tavazzi, S.; Silvestri, L.; Campione, M.; Borghesi, A.; Papagni, A.; Spearman, P.; Yassar, A.; Camposeo, A.; Pisignano, D. *J. Appl. Phys.* **2007**, *102*, 023107. In this reference, RUB unit cell axes were exchanged with respect to ref 3; we maintain a = 26.86 Å, b = 7.19 Å, and c = 14.43 Å.

(22) Laicini, M.; Spearman, P.; Tavazzi, S.; Borghesi, A. *Phys. Rev. B* **2005**, *71*, 0452121.

(23) Laicini, M.; Spearman, P.; Raimondo, L.; Trabattoni, S.; Miozzo, L.; Moret, M. *J. Lumin.* **2004**, *110*, 207.

(24) Mc Intyre, J. D. E.; Aspnes, D. E. *Surf. Sci.* **1971**, *24*, 417.

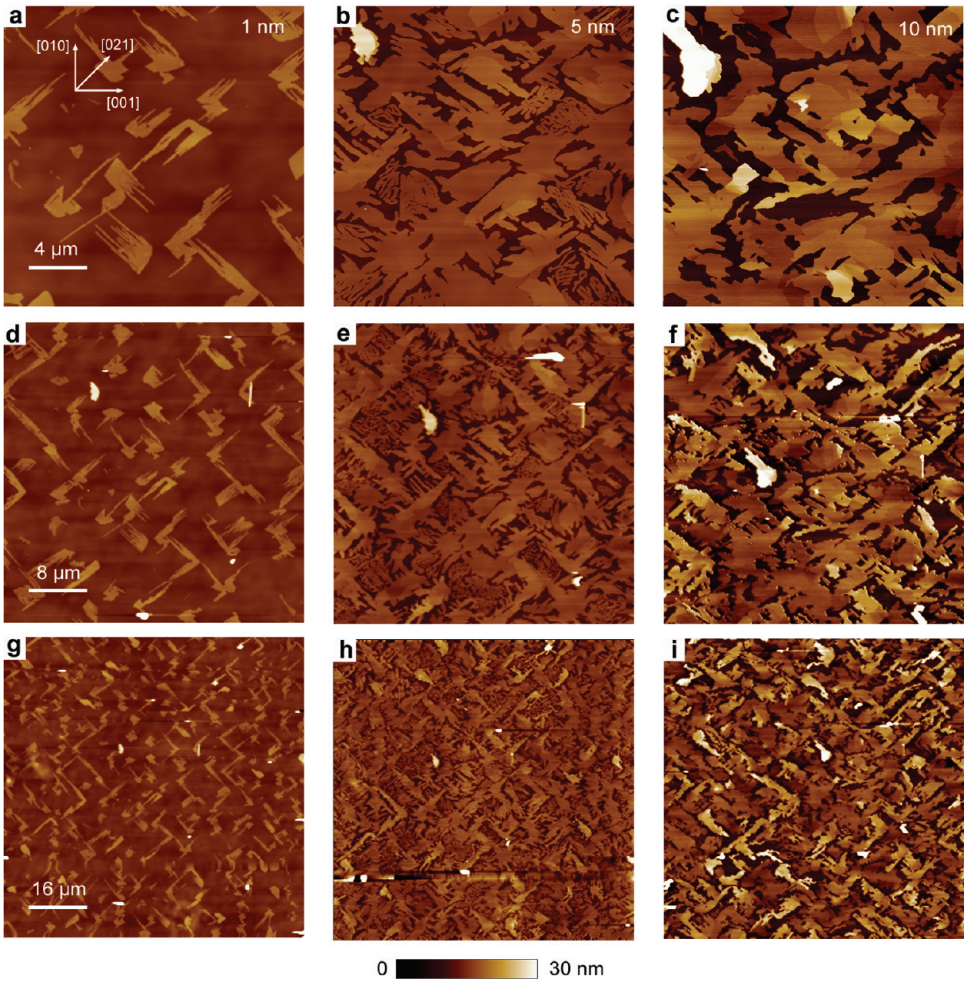

Figure 1. AFM images showing the surface morphology evolution with coverage of the same area for different magnifications of an α-4T thin film deposited on RUB(200). The film nominal thickness is the same for each column and is indicated on the top-right of panels a−c. Notable crystallographic directions of the RUB substrate surface are indicated in the top-left of panel a by white arrows.

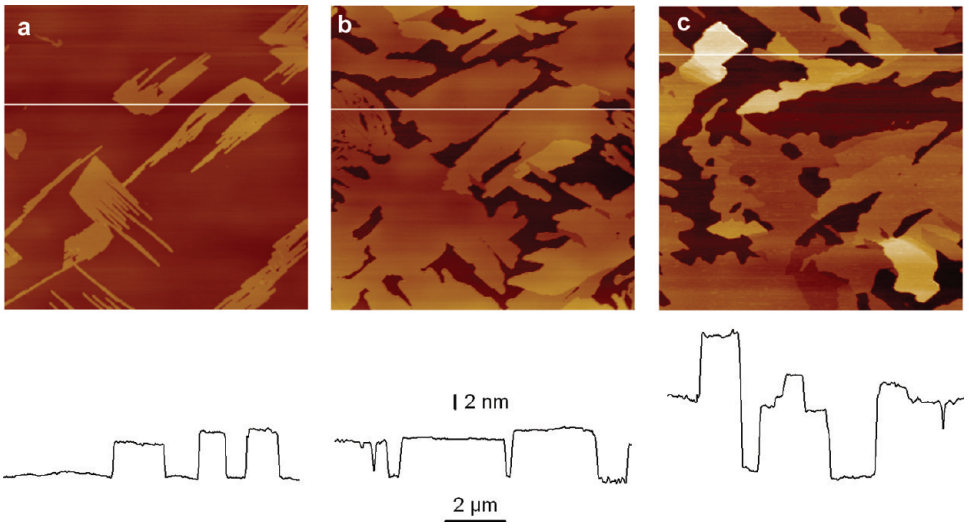

Figure 2. Zoomed AFM images ($10 \times 10\ \mu m^2$) of the areas shown in Figure 1a−c. Below each image, a cross-sectional profile taken along the white line shows the presence of layers with height multiples of the spacing $d_{(002)} = 1.53$ nm between (002) planes in the low-temperature monoclinic polymorph of α-4T.

(i) The similarities between the optical response of the film and an α-4T single crystal (low-temperature polymorph) in the spectral range of its strong optical anisotropy suggest that the α-4T overlayer grows on the RUB-(200) face with α-4T(002) as contact plane.

(ii) The detection of the strong α-4T[100]-polarized optical feature in the spectrum taken with $\delta = 0°$ implies that α-4T[100] is almost parallel to RUB[010], thus defining this as the average dominant orientation of the α-4T film on the RUB substrate.

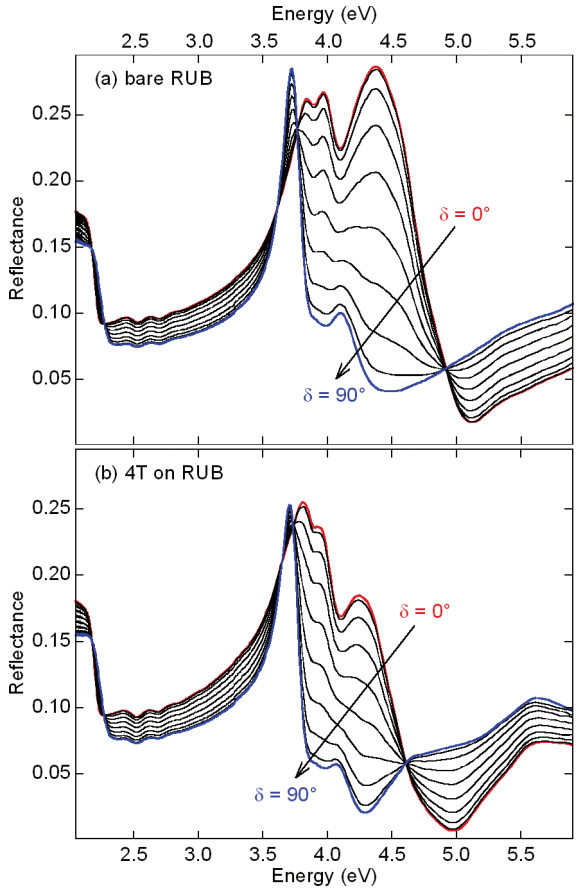

Figure 3. (a, b) Reflectance spectra of the bare RUB substrate and of the α-4T/RUB heterostructure with a 10 nm thickness of the α-4T film, as taken under linearly polarized incident light. The angle of polarization δ is defined by the direction of the electric field of the incident light and RUB[010] and is scanned from 0 to 90° in 10° steps.

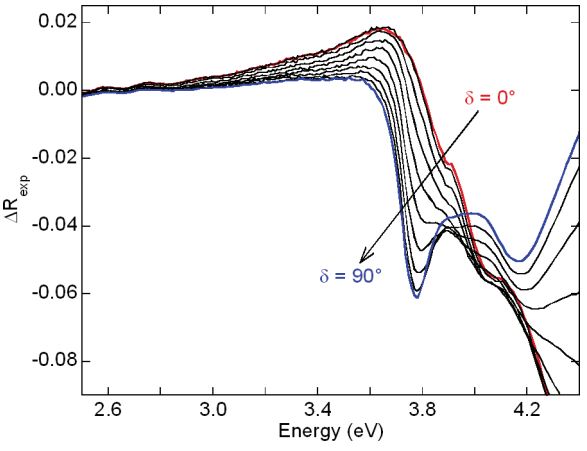

Figure 4. Difference spectra ΔR_{exp} between the spectra of the heterostructure and the bare RUB substrate for the different δ values from 0 to 90°, in 10° steps.

3.2. Microscopic Properties and Epitaxy. For a deeper analysis of the structural properties of the α-4T film in the α-4T/RUB heterostructures, the presence of possible rotational domains can be studied by performing TSM measurements on all the grown films; the results are reported in Figure 5.

The TSM images show that for each coverage, the α-4T islands elongated along the two orthogonal directions RUB[021] and RUB[02$\bar{1}$] display a different contrast: bright for the former and dark for the latter. The clear TSM contrast differentiation of the α-4T islands confirms their crystallinity, while indicating a different azimuthal orientation. Hence, a first morphology−structure relationship arises from this microscopic analysis, indicating that islands elongated along orthogonal directions have different crystallographic orientation.

Fine structural information on the different α-4T domains was obtained by high-resolution AFM measurements on their surface. Figure 6 summarizes the results of such an analysis after processing more than 1000 high-resolution images collected on 5 nm-thick films. By comparing the structure and orientation of the islands with respect to that of the substrate, we identified four rotational domains: every domain has a surface structure with unit cell parameters $a = 6.0 \pm 0.1$ Å and $b = 7.9 \pm 0.2$ Å, corresponding to that of the unreconstructed (002) surface of α-4T ($a = 6.09$ Å $b = 7.86$ Å).[13] The superposition of the Fourier spectra obtained from the contrast of atomic-scale images collected on α-4T domains and on the RUB bare surface shows that the aforementioned orientations arise from the coincidence of the non primitive reciprocal lattice vectors α-4T⟨110⟩ and RUB⟨012⟩ (see the Supporting Information, Figure S2). The detected coincidence gives rise to four different azimuthal orientations at $\theta = \pm 7.32°$ and $\theta = \pm 82.68°$ (hereinafter approximated as $\theta = \pm 7°$ and $\theta = \pm 83°$), θ being the angle between α-4T[100] and RUB[010], as calculated from X-ray crystallographic data.[3,13] The possible difference in population of these four domains is sufficiently small to make likely their imaging by random tip positioning (see below).

Domains appearing with the same bright contrast in TSM images are observed to be oriented either at $\theta = +7°$ or $\theta = +83°$ (Figure 6a and c), whereas domains appearing with the same dark contrast in TSM images are observed to be oriented either at $\theta = -7°$ or $\theta = -83°$ (Figure 6b and d). These findings can be explained considering that the TSM signal as a function of θ has a 180° periodicity, which, considering the symmetry of the α-4T(002) surface, is expected to vanish when the scan direction is parallel either to α-4T[100] or to α-4T[010].[16] Additionally, considering that the four orientations at ±7° and ±83° are symmetrical with respect to the scan direction, the TSM contrast of domains at $\theta = +7°$ is found to be the same as that of domains at $\theta = +83°$ (and the TSM contrast of domains at $\theta = -7°$ is the same as that of domains at $\theta = -83°$), as indeed expected.

It must be remarked that all the results of TSM and atomic-scale AFM reported above are obtained probing the topmost layer of α-4T islands, which on average are composed of three molecular layers. The eventual presence of strain and defects in the first layer in contact with the substrate are therefore not demonstrated; however, in the case of Volmer−Weber growth of islands with relatively large lattice mismatch (see section 3.3), the inference of the structure of the first layer from that of the successive relaxed layer is quite reasonable.

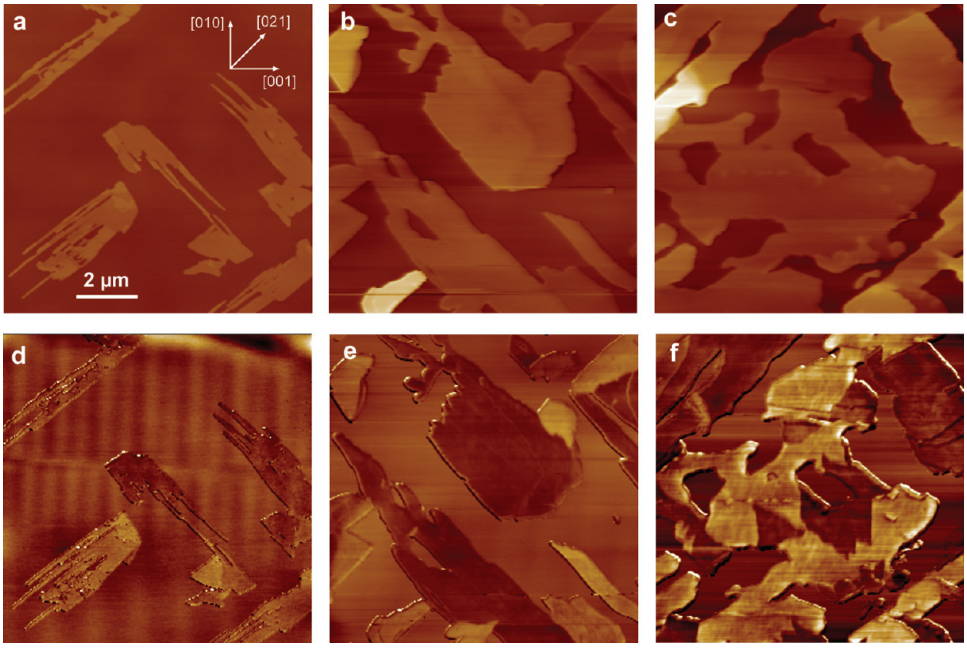

Figure 5. (a−c) Contact-mode AFM and (d−f) corresponding TSM images of α-4T films with nominal thickness (a) 1, (b) 5, and (c) 10 nm. Notable crystallographic directions of the substrate surface are indicated in the top-right of panel a by white arrows. The TSM data are collected during the tracing of the tip from left to right.

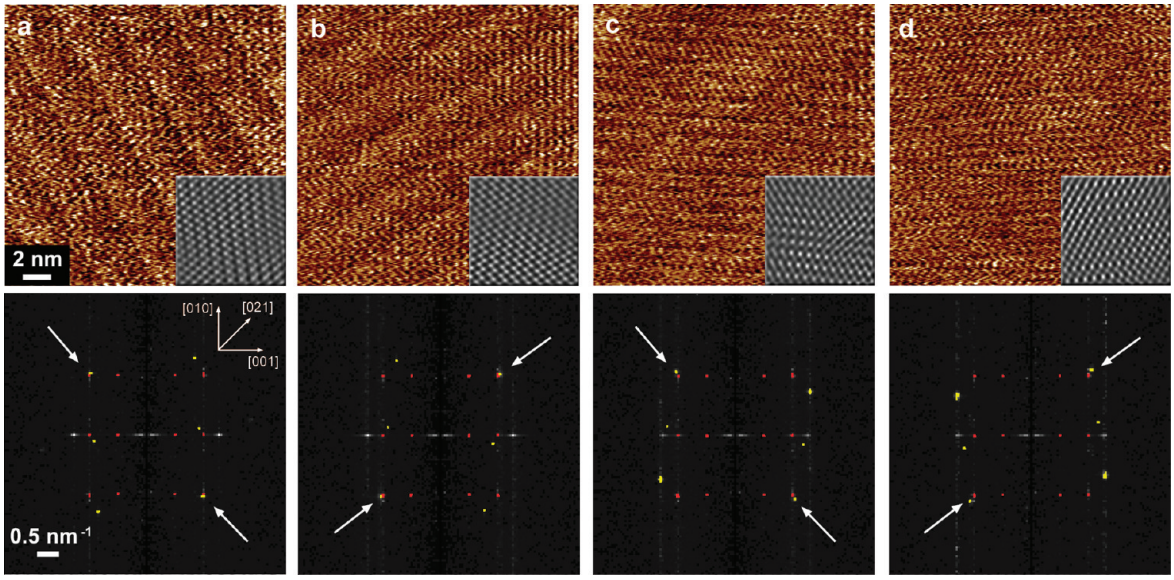

Figure 6. Atomic-scale AFM images taken on α-4T crystalline domains on RUB(200) with four different azimuthal orientations. In the insets, the Fourier filtered images are reported, showing the orientation of the surface rectangular unit cell (*a*, short axis; *b*, long axis; see the Supporting Information, Figure S2). Below each image, the corresponding 2D Fourier transform (yellow) is superimposed with that obtained from a high-resolution image collected on the bare RUB surface (red). White arrows highlight coincident reciprocal lattice points. The orientation of the substrate is the same for each image and is indicated in the top-right corner of the spectrum in panel a.

A further relevant step for a microscopic description of the α-4T/RUB heterostructures is the study of epitaxy: the starting point, and the simplest as well, is represented by lattice misfit calculation. A common tool for performing such an analysis is represented by Epicalc,[25] based on an algorithm that considers only the geometry (lattice parameters) of the substrate-overlayer interface. The output function (V/V_0) presents minima at the azimuthal angle θ when some coincidence between substrate and overlayer lattice points occurs. In the case of the α-4T(002)/ RUB(200) interface, there is no θ value between α-4T[100] and α-4T[010] at which V/V_0 provides a significant negative peak (Figure 7a). Only if one performs the calculation starting with a 3 × 3 overlayer supercell, i.e., neglecting the unfavorable position of 3/4 of the totality of lattice points, does one find a coincidence ($\Delta V/V_0 > 0.5$) at $\theta = \pm 37.8°$, and other less meaningful minima at $\theta = \pm 23.2°$ and $\theta = \pm 52.3°$, none of them having any relation with the experimental findings.

(25) Hillier, A. C.; Ward, M. D. *Phys. Rev. B* **1996**, *54*, 14037. Downloadable software at http://www.nyu.edu/fas/dept/chemistry/wardgroup/Software.html.

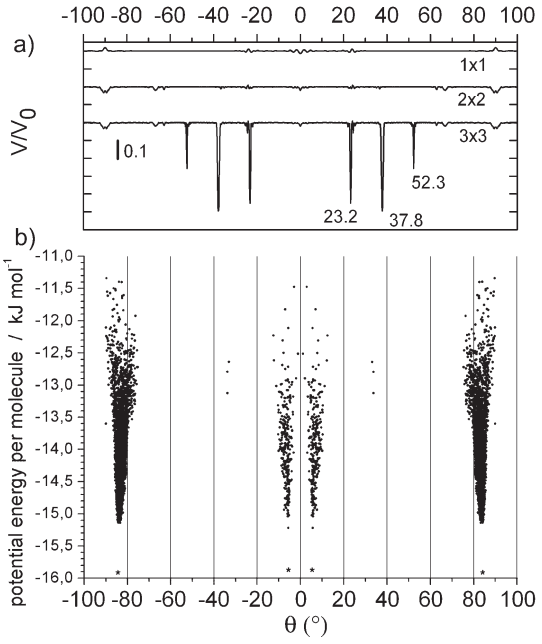

Figure 7. (a) Geometric coincidence calculated with the program Epicalc for a α-4T(002) overlayer on RUB(200). The azimuthal positions of negative peaks (coincidences) in the adimensional potential V/V_0 are indicated as a function of the overlayer supercell dimension: 1×1, 2×2, and 3×3 (baselines, corresponding to $V/V_0 = 1$, are offset for clarity). (b) Results of empirical force field calculations showing the potential energy for many different in-plane alignments of (002)-oriented α-4T epitaxial islands made up of 39 molecules. The asterisks below the minima indicate the azimuth and energy obtained after minimization.

The interactions between the atomic arrangements emerging at the substrate and overlayer surfaces must be responsible for organic−organic heteroepitaxy even in the absence of a good matching of lattice parameters. Azimuthal orientations which give a reasonable potential energy for the substrate/overlayer interaction were located by means of docking runs with an overlayer model crystallite free to move and interact with the substrate; this method was successful in explaining the occurrence of two azimuthal orientations of *p*-sexyphenyl on KAP.[26] Empirical force field potentials and bulk terminated α-4T(002) and RUB(200) surfaces were employed.

The interface of the heterostructure shows a potential energy strongly dependent on the azimuthal orientation of the α-4T(002) crystal with respect to the RUB(200) (Figure 7b). The potential energy shows two well-defined and populated energy minima peaks centered at ca. 7° and 83° for the azimuthal rotation of α-4T[100] vs RUB[010] (i.e., θ), in full agreement with the epitaxial relations extracted from AFM data. After minimization, these two energy minima are found at azimuths $\theta = \pm 5.46°$ and $\theta = \pm 84.27°$, corresponding to energies of −15.87 and −15.91 kJ/mol per molecule, respectively. For this reason, the number of simulated points defining the two energy minima in Figure 7b is not related to the population of domains and reflects only the ease of access of each configuration by means of the genetic algorithm adopted.

Another feature found in our simulations is the low value of the tilt angle between the normals to the substrate and overlayer surfaces, the energy minima being reachable only for a maximum deviation of ca. 2° (data not shown).

Given the detected presence of four rotational domains, one should discuss in more detail the spectroscopic results, with the aim to provide some indications on the relative domain population. We therefore performed a simulation of the reflectance spectra of the whole heterostructure by considering a three-layer system composed by air/α-4T/RUB,[27] with a semi-infinite RUB substrate and a 10 nm thick (002)−oriented α-4T film. For simplicity, in our simulation, we approximated the response of the four domains at $\theta = \pm 7°$ and $\theta = \pm 83°$ with that of only two domains at $\theta = 0°$ and $\theta = 90°$ (literature data were considered for the dielectric functions of α-4T and RUB single crystals).[21−23] Figure 8a,b reports the calculated difference spectra (ΔR_{calc}, continuous curves) for $\theta = 0$ and 90° considering the two directions of light polarization $\delta = 0$ and 90°, being the most meaningful for describing the heterostructure optical response. For energy up to about 3.7 eV, both couples of calculated spectra are very similar to the experimental ones (ΔR_{exp}, dotted curves), but at higher energy, some difference can be observed. Looking at the overall line shape of experimental and calculated spectra, the conclusion that the preferential orientation is $\theta = 0°$ can therefore be proposed.

A few comments can be added looking at Figure 8a in more detail: even though an overall good agreement is found between experiment and simulation for one of the azimuthal orientation, some difference in the spectral line shape of the simulated and the experimental spectra exists. Indeed, looking at the $\delta = 90°$ spectra, a substantially negative slope of the calculated curve can be observed until about 3.7 eV, which does not satisfactorily reproduce the experimental (slight) positive slope in ΔR_{exp}. One reason could lie in the use of the calculated α-4T dielectric tensor of ref 20 which neglects contributions from charge-transfer states in the range between 3 and 3.5 eV,[28] which nonetheless would be too small to justify the observed difference. A definitive explanation comes from the fact that a non-negligible amount of domains oriented following the epitaxial relation $\theta = 90°$ exists and affects the optical response. To check this, the simulated spectra in Figure 8c correspond to samples where the two rotational domains coexist, with surface coverage $S_{\theta = 0°}$ and $S_{\theta = 90°} = 1 - S_{\theta = 0°}$, respectively. By adding some domains at $\theta = 90°$, the calculated spectra for both polarizations better approximate the experimental ones. In particular, considering $S_{\theta = 0°} = 0.75$, i.e., 25% of the domains oriented at $\theta = 90°$ (dotted curves), the spectrum at $\delta = 90°$ shows a lower negative slope, approaching the experimental curve; at the same time, the spectrum for $\delta = 0°$ presents a lower peak intensity, also

(26) Haber, T.; Resel, R.; Thierry, A.; Campione, M.; Sassella, A.; Moret, M. *Physica E* **2008**, *41*, 133.
(27) Born, M.; Wolf, E. *Principles of Optics*; Pergamen Press: Oxford, U.K., 1980.
(28) Tavazzi, S.; Laicini, M.; Raimondo, L.; Spearman, P.; Borghesi, A.; Papagni, A.; Trabattoni, S. *Appl. Surf. Sci.* **2006**, *253*, 296.

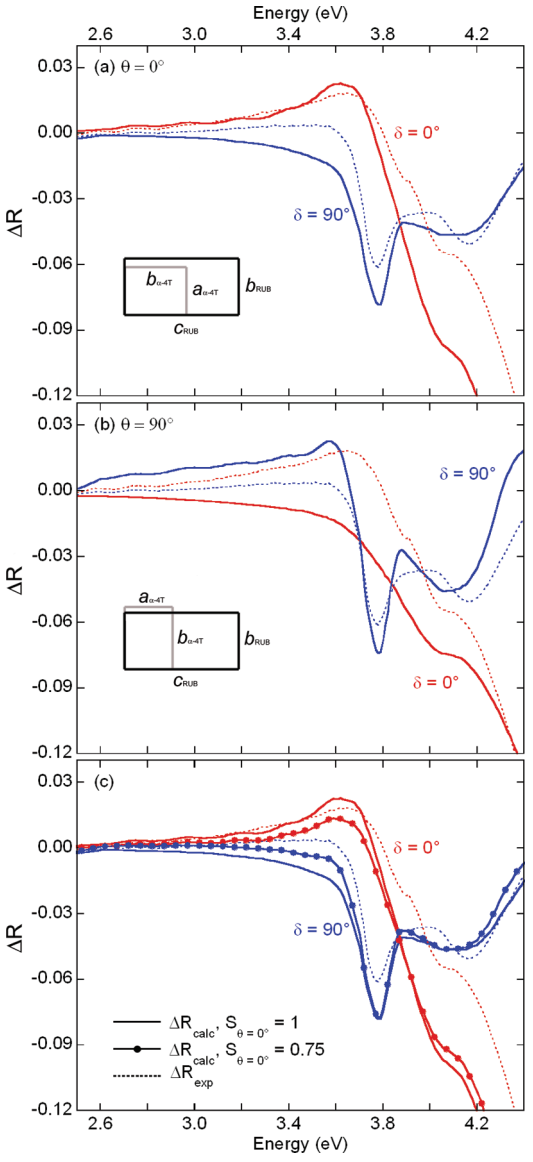

Figure 8. (a, b), Comparison of experimental and simulated ΔR spectra (dotted and continuous curves, respectively), as calculated by considering the two azimuthal orientations, i.e., $\theta = 0$ and $\theta = 90°$, sketched in the insets; (c) Comparison of experimental and simulated ΔR spectra as calculated for different relative populations of the two domains. In all panels the spectra for $\delta = 0°$ polarization are in red and for $\delta = 90°$ polarization are in blue.

in better agreement with the experimental curve (which includes the contribution from charge-transfer states). In this way, the difference between the two polarizations at 3.6 eV in the experimental spectra is nearly matched. Finally, it should be noted that by further increasing $S_{\theta = 90°}$ the two spectra do not present such a difference (see the Supporting Information, Figure S3).

3.3. Concluding Remarks. Considering all the results on the microscopic and macroscopic characteristics of the α-4T epitaxial films on RUB, several conclusions are drawn. Despite the absence of commensurism (see Figure 7a), Figure 6 demonstrates that the α-4T overlayer assumes four well-defined orientations, in accordance with the epitaxial relation α-4T⟨110⟩ // RUB⟨021⟩, fully supported by force field calculations (see Figure 7b). When coincidence of nonprimitive reciprocal lattice

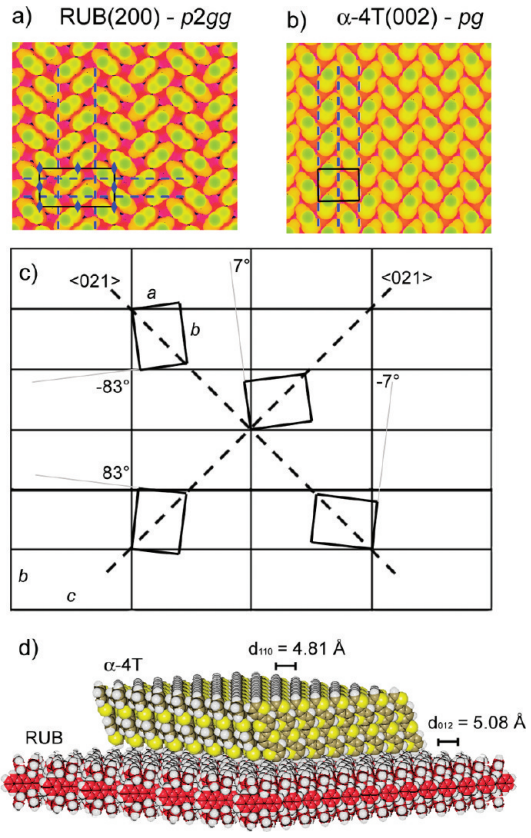

Figure 9. (a, b) Structural models with depth-dependent color scale of the RUB(200) and α-4T(002) unreconstructed surfaces. The plane group symmetry deduced from the symmetry operators superimposed in the model is reported. The surface unit cell is represented by a rectangular box with black lines. (c) Azimuthal orientations of the (002)-oriented α-4T overlayer corresponding to the line-on-line epitaxial relation α-4T ⟨110⟩ // RUB⟨021⟩ deduced from the AFM analysis. (d) Structural model of the α-4T/RUB heterostructure with the experimentally observed epitaxial relation (viewed along α-4T[110] and RUB[021]), evidencing the matching of the main surface corrugations of the two semiconductors.

vectors occurs, the epitaxial relation is defined as line-on-line.[10] This type of epitaxial relation has been observed only in the case of organic heterojunctions and has recently been demonstrated to characterize the interface of RUB thin films deposited on tetracene single crystals.[29] It is remarkable that even though it represents the weakest form of epitaxy, in this latter case, the line-on-line relation corresponds to an overlayer with a unique orientation, i.e., having no rotational domains. The formation of rotational domains, as those in the α-4T/RUB heterostructures of the present work, is related to the symmetry of the substrate and overlayer surfaces.

Looking in more detail at the surfaces, in Figure 9a the RUB(200) surface is observed to be lined up with hydrogen atoms bonded to the lateral phenyl rings of the molecules; the surface corrugation allows one to recognize the presence of both 2-fold axes of rotation and glide planes (dashed lines), giving an overall plane symmetry corresponding to *p2gg*. On the other hand, the α-4T(002) surface (Figure 9b) is lined up with hydrogen atoms in α position of the terminal oligothienyl units, giving rise to a surface corrugation where only glide planes oriented

(29) Campione, M. *J. Phys. Chem. C* **2008**, *112*, 16178.

parallel to the α-4T[100] direction (or $a_{\alpha\text{-}4T}$-axis) can be identified, separated by half a unit cell. This condition corresponds to a *pg* plane symmetry. Furthermore, the $a_{\alpha\text{-}4T}$-axis is a polar axis, since, as can be observed in Figure 9b, the α-4T[100] direction is not equivalent to the α-4T[$\bar{1}$00] one. In Figure 9c, one can observe the relative orientation of the surface lattice of the α-4T overlayer and the RUB substrate in the four domains. Note that each orientation, because of the polarity of the *a*-axis, represents two nonequivalent domains rotated by 180° one another. However, because of the inability of AFM to distinguish such rotational domains, we can not demonstrate their presence. The two couples of domains at $\theta = \pm 7°$ and at $\theta = \pm 83°$ are predicted by the force field calculation reported in Figure 7 to have the same interface energy; however, the simulations of the optical spectra reported in Figure 8 show that a prevalence (ca. 75%) of domains at $\theta = \pm 7°$ is present. This prevalence may arise from an actual difference of interface energy establishing during the nucleation stage, which docking simulations based on rigid models are not able to predict.

Finally, the physical rationale behind the selection of these peculiar orientations is still to be explained. By observing Figure 9c one realizes the coincidence of the α-4T⟨110⟩ and RUB⟨021⟩ directions. The α-4T⟨110⟩ directions run parallel to rows of first nearest-neighbors of close-packed molecules (see Figure 9b): this gives rise to a strong corrugation of the α-4T(002) surface along an orthogonal direction having a periodicity equivalent to $d_{110} = 4.81$ Å (see Figure 9d). Analogously, the RUB⟨021⟩ directions run parallel to well-defined rows of protruding hydrogen atoms (Figure 9a), giving rise to a pronounced corrugation with periodicity corresponding to $d_{012} = 5.08$ Å (see Figure 9d where the molecular arrangement at the interface of the heterostructure is sketched). Hence, the coincidence of direction and periodicity (misfit 5.3%) of the main surface corrugations of the two materials drives the orientation of the overlayer.

The furrows running along RUB⟨021⟩ also have a dramatic influence on the diffusion processes of the deposited molecules. This affects the properties of the heterostructures over a much larger scale, as can be observed from Figure 1, where almost all islands show an elongated shape parallel to RUB⟨021⟩, sometimes having long fringes, giving rise to a peculiar morphological texture of the film. It is worth noting how this morphology, driven by interface energy and growth kinetics, differs from the equilibrium shape of crystalline α-4T,[30] which is tabular with well-developed (100) and (010) faces.

(30) Campione, M.; Sassella, A.; Moret, M.; Marcon, V.; Raos, G. *J. Phys. Chem. B* **2005**, *109*, 7859.

4. Conclusions

Given the complete microscopic picture of the surface and interface properties of the α-4T/RUB heterostructures and considering their morphology and optical properties, some insights on the relationship between growth, structure, and macroscopic behavior can be obtained. At a first level, the overlayer has been found to be crystalline over a macroscopic scale and with a clear textural order; this is also reflected by the optical properties, which display a clear anisotropy of the heterostructure and permit determining the alignment directions of the overlayer on the substrate; this also gives an indication of the relative population of the different orientations. At a second level of understanding, a precise preferential azimuthal orientation of the domains has been found over a microscopic scale and interpreted in terms of surface symmetry and local adhesive properties. Indeed, the coincidence of the main surface corrugations of the two materials forming the heterostructure drives the orientation of the overlayer into four rotational domains.

The growth of well-oriented heterojunctions of organic semiconductors is an important step toward the optimization of the performance of devices such as solar cells, where interface properties dominate the dynamics of charge separation. The results obtained combining α-4T and RUB provide important guidelines for predicting the interface structure of two systems with apparently incommensurate structures, which are very common in the field of organic semiconductor crystals. Furthermore, these results elucidate the surface properties of crystalline RUB, one among the organic semiconductors with the most promising applications. The peculiar corrugation of its crystalline surface gives rise to an interesting propensity to induce an oriented growth of other organic materials. This prerogative can be exploited for the growth of multilayer structures and superlattices.

Acknowledgment. This work was supported by Fondazione Cariplo (Grant 2007/5205).

Supporting Information Available: α-Quaterthiophene single crystal vs α-quaterthiophene thin film optical response, indexation of 2D fast Fourier transforms of atomic-scale AFM images, simulations of optical spectra (PDF). This material is available free of charge via the Internet at http://pubs.acs.org.